


Enhancing schistosomiasis drug discovery approaches with optimized proteasome substrates

Elany B. Silva^{1,2} | Zhenze Jiang¹ | Chenxi Liu¹ | Pavla Fajtová¹ |
 Thaiz R. Teixeira¹ | Giovana de Castro Fiorini Maia² | Lawrence J. Liu¹ |
 Nelly El-Sakkary¹ | Danielle E. Skinner¹ | Ali Syed¹ | Steven C Wang¹ |
 Conor R. Caffrey¹ | Anthony J. O'Donoghue¹ 

¹Center for Discovery and Innovation in Parasitic Diseases, Skaggs School of Pharmacy and Pharmaceutical Sciences, University of California San Diego, La Jolla, California, USA

²Department of Biochemistry & Immunology, Federal University of Minas Gerais, Belo Horizonte, Brazil

Correspondence

Conor R. Caffrey and Anthony J. O'Donoghue, Center for Discovery and Innovation in Parasitic Diseases, Skaggs School of Pharmacy and Pharmaceutical Sciences, University of California San Diego, 9255 Pharmacy Lane, MC 0657, La Jolla, CA 92093, USA.
 Email: ccaffrey@health.ucsd.edu;
ajodonoghue@health.ucsd.edu

Funding information

National Institute of Allergy and Infectious Diseases, Grant/Award Numbers: R01AI158612, R21AI133393, R21AI146387, R21AI171824; H2020 Marie Skłodowska-Curie Actions, Grant/Award Number: 846688; Akademie Věd České Republiky, Grant/Award Number: MSM200551901

Review Editor: John Kuriyan

Abstract

Schistosomiasis, a neglected tropical disease infecting over 200 million people globally, has limited therapeutic options. The 20S proteasome is a validated drug target for many parasitic infections, including those caused by *Plasmodium* and *Leishmania*, and we have previously demonstrated antischistosomal activity with inhibitors targeting *Schistosoma mansoni* 20S proteasome (Sm20S). Here, we developed optimized subunit-specific substrates for Sm20S based on data generated by Multiplex Substrate Profiling by Mass Spectrometry (MSP-MS). These substrates exhibit 9-fold or more improved activity compared to traditional human constitutive 20S proteasome (c20S) substrates. The optimized substrates also eliminated the need for extensive Sm20S purification, as robust enzyme activity could be detected in parasite extracts following an ammonium sulfate precipitation step. Finally, we show that the substrate and inhibition profiles for the 20S proteasome from the three medically important schistosome species are similar. This suggests that Sm20S-focused inhibitor development can be efficiently extrapolated to the other schistosome species, leading to significant time and resource savings.

KEYWORDS

drug discovery, drug target, MSP-MS, neglected disease, parasite, protease inhibitor, proteasome, *Schistosoma*, schistosomiasis, substrate profile, substrate specificity

1 | INTRODUCTION

Schistosomiasis, also known as bilharzia, is a neglected tropical disease caused by blood flukes of the *Schistosoma* genus. This debilitating illness thrives in areas lacking safe drinking water and sanitation, and the World Health Organization estimates 251.4 million

people are in need of treatment (WHO 2023). Three main species, *Schistosoma mansoni*, *Schistosoma haematobium* and *Schistosoma japonicum*, are responsible for human schistosomiasis. Adult worms in the bloodstream release eggs that become lodged in organs like the spleen, liver, intestine, and/or bladder. These eggs trigger chronic inflammation and fibrosis, leading to fatigue, pain, and disability. The resulting lost school days for children and reduced worker

Elany B. Silva, Zhenze Jiang, and Chenxi Liu are co-first authors.

productivity create a vicious cycle, whereby schistosomiasis both perpetuates and stems from poverty (Colley et al. 2014; McManus et al. 2018; Verjee 2019).

Praziquantel (PZQ) has been the cornerstone of schistosomiasis treatment and control since the early 1980s (Andrews et al. 1983; Caffrey 2015; Caffrey et al. 2019), and is primarily delivered via mass drug administration programs to reduce disease burden at the community level (Mwanga et al. 2020). Although reasonably effective at the standard single 40 mg kg⁻¹ oral dose (Cioli et al. 2014; Fukushige et al. 2021; Hailgebriel et al. 2021; Zwang and Olliaro 2017), PZQ has several pharmacological and pharmaceutical limitations. These include incomplete efficacy across all parasite growth stages, a racemic composition that renders half the dose inactive (contributing to large, unpleasant-tasting tablets), and rapid metabolism to inactive components such that exposure of the parasite to the parent active ingredient is brief (Badoco et al. 2022; Caffrey 2015; Caffrey et al. 2019; Cioli et al. 2014; Danso-Appiah et al. 2022; Gryseels et al. 2001; Sabah et al. 1986; Wolfe et al. 2018). Furthermore, the threat of drug resistance is ever-present (Melman et al. 2009; Summers et al. 2022). Consequently, these PZQ-related drawbacks have spurred the search for new drugs.

Among the potential molecular drug targets discussed over the years for chemotherapy of schistosomiasis, a more recent addition has been the

proteasome (Bibo-Verdugo et al. 2017; Bibo-Verdugo et al. 2019; do Patrocinio et al. 2020) which is an evolutionarily conserved, multi-subunit, ATP-dependent proteolytic complex that is vital to cellular proteostasis (Bard et al. 2018; Sahu and Glickman 2021). Each 20S proteasome core comprises two stacked rings of seven β subunits between two rings of seven α subunits. Among the seven β subunits in each ring, three (β 1, β 2, and β 5) are proteolytically active (Figure 1a), and, based on their peptidyl cleavage specificities, are described as having caspase-, trypsin-, and chymotrypsin-like specificities, respectively. The 20S proteasome is often associated with 19S regulatory particles at one or both ends, forming the 26S or 30S proteasome, respectively. Proteins identified for degradation are ubiquitinated and then recognized by the 19S regulatory particle. The proteins are unfolded in an ATP-driven process and then threaded into the 20S proteolytic core for degradation into short peptides. The human constitutive 20S proteasome (c20S) is a well-established target for various cancers, and the US Food and Drug Administration has approved three small-molecule inhibitors, bortezomib (BTZ) (Chen et al. 2011), carfilzomib (CFZ) (Groen et al. 2019), and ixazomib (IXZ) (Ramirez 2017). These drugs preferentially target β 5; however, at higher concentrations, BTZ and IXZ also inhibit β 1 while CFZ inhibits β 2 (Altun et al. 2005; Augello et al. 2018; Schots et al. 2012). In addition, the marine natural product, marizomib (MZB),

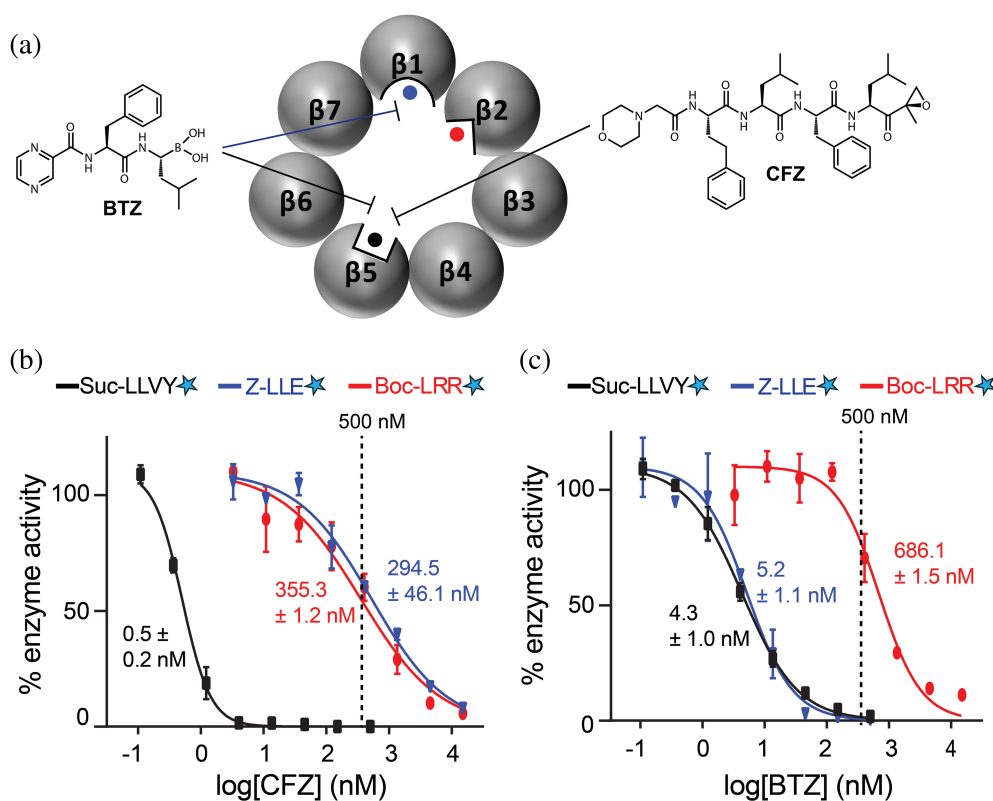


FIGURE 1 Determining the inhibitor concentration needed to inactivate Sm20S β 5 or β 5/ β 1 subunits. (a) Schematic representation of the β -ring of Sm20S showing the β 1, β 2, and β 5 catalytic subunits with differently shaped active sites to illustrate differences in inhibitor specificity. Also shown are the chemical structures of BTZ and CFZ, and the Sm20S subunits that each preferentially inhibits. (b, c) The inhibition potency of CFZ and BTZ was measured for each catalytic subunit using Z-LLE-amc for β 1, Z-LRR-amc for β 2, and Suc-LLVY-amc for β 5. The light blue star represents the amc fluorophore. Assays were performed in technical triplicate.

is a brain-penetrable proteasome inhibitor that preferentially targets the $\beta 5$ subunit but also inhibits $\beta 1$ and $\beta 2$ at higher concentrations (Potts et al. 2011). MZB is in phase 3 clinical trials for the treatment of glioblastoma (Bota et al. 2021).

Despite being evolutionarily conserved, key differences between human and parasite proteasomes have been identified and exploited to develop selective inhibitors (Bennett et al. 2023; Bibo-Verdugo et al. 2019; LaMonte et al. 2017; Lawong et al. 2024; Li et al. 2016; Liu et al. 2024a; Nagle et al. 2020; O'Donoghue et al. 2019; Robbertse et al. 2024; Wyllie et al. 2019), the most prominent of which are two drug candidates (GSK245 and LXE408) currently undergoing clinical trials for leishmaniasis (Nagle et al. 2020; Wyllie et al. 2019). Potent inhibitors of the *Plasmodium falciparum* proteasome (Pf20S) have been identified using various approaches, such as analyzing how the proteasome processes specific substrates (cleavage profiling) (Li et al. 2016) and the screening of potential inhibitor libraries (Kirkman et al. 2018; Li et al. 2012; Xie et al. 2018). These efforts have yielded covalent inhibitors incorporating different chemical reactive groups (epoxyketone (Almaliti et al. 2023; LaMonte et al. 2017), vinyl sulfone (Yoo et al. 2018), or boronic acid (Xie et al. 2018)) with selectivity indices of up to 2640 between parasite and human cells. Our own research has focused on synthesizing analogs of carmaphycin B, a marine natural product containing the epoxyketone group, resulting in compounds that are effective in a mouse model of malaria (Almaliti et al. 2023; LaMonte et al. 2017).

We previously demonstrated that targeting the *S. mansoni* 20S (Sm20S) in vitro with proteasome inhibitor drugs approved for cancer treatment leads to immobility and, ultimately, fatal degenerative changes in the adult worm (Bibo-Verdugo et al. 2017). In addition, using a small collection of carmaphycin B analogs, we identified carmaphycin-17 as a hit compound that decreased worm mobility by >95% after 24 h at 1 μ M while also having a 27-fold lower cytotoxicity to HepG2 cells relative to carmaphycin B (Bibo-Verdugo et al. 2019). This suggests that a path forward exists to build carmaphycin B-based inhibitors with greater specificity for the Sm20S compared to the c20S anti-target.

Here, we describe the purification of Sm20S and define its substrate cleavage specificities using Multiplex Substrate Profiling by Mass Spectrometry (MSP-MS) (Small et al. 2013). MSP-MS is a rapid, simple, and versatile mass spectrometry-based peptide digestion assay used to detect and quantify proteolytic activity (Lapek et al. 2019; O'Donoghue et al. 2012; Rohweder et al. 2023). It consists of a substrate library of 228 synthetic 14-mer peptides with high sequence diversity and a total of 2964 cleavable bonds. This assay has been used to uncover the substrate specificity of numerous endoproteases and exopeptidases

from bacteria, fungi, insects, and mammalian cells (Beekman et al. 2018; Jiang et al. 2021; Lysyk et al. 2021; Maffioli et al. 2020; O'Donoghue et al. 2015; O'Donoghue et al. 2025; Small et al. 2013). MSP-MS has also been used to uncover the proteolytic activity of c20S, in addition to the human immunoproteasome and the *Trichomonas vaginalis* proteasome (Fajtova et al. 2024; Winter et al. 2017). In this study, we used MSP-MS to reveal that each of the Sm20S catalytic subunits cleaves at distinct sites within the peptide library, therefore revealing that Sm20S has three distinct substrate recognition sites. The data arising from this study were then used to design fluorogenic peptidyl substrates that are each specific for the three proteolytically active subunits. We show that each new substrate is more efficiently cleaved by Sm20S compared to the c20S substrates that were previously used (Bibo-Verdugo et al. 2019). Part of this process involved developing a method to measure Sm20S proteolysis in extracts. Last, we demonstrate that the rate of cleavage for the new substrates is similar between the three schistosome species most responsible for human disease. This suggests that a single campaign of inhibitor development focusing on Sm20S may be sufficient to develop a pan-schistosomicide, consistent with the target product profile for schistosomiasis (Caffrey 2007; Caldwell et al. 2023).

2 | METHODS

2.1 | Preparation of schistosomes

The acquisition and preparation of mixed-sex adult *S. mansoni* have been described (Abdulla et al. 2007; Abdulla et al. 2009). The Naval Medical Research Institute (NMRI) isolate of *S. mansoni* was cycled between *Biomphalaria glabrata* snails and male Golden Syrian hamsters (infected at 4–6 weeks of age) as intermediate and definitive hosts, respectively. In brief, adult schistosomes were harvested from hamsters 42 days post-infection in RPMI or DMEM and washed five times prior to maintenance overnight at 37°C and 5% CO₂ in Basch medium (Basch 1981) containing 4% heat-inactivated FBS, 100 μ g mL⁻¹ streptomycin, and 100 U mL⁻¹ penicillin. Worms were then washed five times in RPMI or DMEM prior to freezing at -80°C. The use of small vertebrate animals was approved by the Institutional Animal Care and Use Committee (IACUC) of the University of California San Diego. UCSD-IACUC derives its authority for these activities from the United States Public Health Service (PHS) Policy on Humane Care and Use of Laboratory Animals, and the Animal Welfare Act and Regulations (AWAR). Frozen, mixed-sex adult *S. haematobium* and *S. japonicum* adult worms were provided to us by the Schistosomiasis Resource Center at the Biomedical

Research Institute, Rockville, MD, USA (www.beiresources.org).

2.2 | Purification of the *S. mansoni* 20S proteasome (Sm20S)

Adult, mixed-sex *S. mansoni* worms were washed and homogenized using a motorized Teflon pestle in 1.5 mL tubes containing ice-cold 100 mM Tris-HCl, 100 μ M E-64, pH 7.5. Protein extracts were centrifuged for 15 min at 14,000 *g* and 4°C, and the supernatant was subjected to two ammonium sulfate precipitation steps on ice at 30% and 60% saturation, respectively, each for 60 min. After centrifugation for 15 min at 14,000*g* and 4°C, the supernatant was discarded, and the precipitated proteins were resuspended in ice cold 100 mM Tris-HCl, pH 7.5, 100 μ M E-64. The samples were enriched for Sm20S when concentrated using 100 kDa centrifugal filter units (Amicon). Protein concentration was quantified using the Pierce BCA kit.

Samples were either used for enzyme assays (defined as Sm20S-enriched) or subjected to column chromatography for Sm20S purification. For the latter, samples were loaded onto a Superose 6 10/300 gel filtration column under the control of an ÄKTA Pure instrument (GE Healthcare Life Sciences). Proteins were eluted using 50 mM HEPES, 10% glycerol, 0.125M NaCl, pH 7.5. Fractions of 0.5 mL were collected and assayed for proteasome activity with 25 μ M Succinyl-Leu-Leu-Val-Tyr-7-amino-4-methylcoumarin (Suc-LLVY-amc) in assay buffer (50 mM Tris, 0.02% SDS, pH 7.5). The assay was performed at 24°C using a Synergy HTX multi-mode reader (ex/em = 360 nm/460 nm; BioTek Instruments). Fractions containing proteasome activity were pooled and loaded onto a 5-mL anion exchange HiTrap DEAE FF column (Sigma). Proteins were eluted using 50 mM HEPES, 10% glycerol, pH 7.5, and a linear gradient of 0.125 to 0.6M NaCl. Fractions (1.5 mL) were collected and assayed with Suc-LLVY-amc as described above. Fractions containing proteasome activity were pooled, concentrated using a 100 kDa centrifugal filter unit (Amicon), and stored at -80°C.

2.3 | Concentration-response assays

CFZ and BTZ were dissolved in 100% DMSO to a final concentration of 10 mM. Each compound was then 3-fold serially diluted 10 times in 100% DMSO such that the concentration ranged from 3.33 mM to 169 μ M. Each dilution was then further diluted 250-fold in 20 mM Tris-HCl pH 7.5, 0.02% SDS containing 20 nM Sm20S. The enzyme and inhibitor were preincubated for 15 min, and then 15 μ L was added into 9 wells on a 384-well plate containing either 15 μ L 20 μ M Suc-LLVY-amc, 20 μ M Boc-LRR-amc, or 20 μ M Z-LLE-amc in 20 mM

Tris-HCl pH 7.5, 0.02% SDS. The final concentration of enzyme and substrate in each well was 10 nM and 10 μ M, respectively, while the final inhibitor concentration ranged from 740 to 0.3 nM for the most potent inhibitors and 20 μ M to 9 nM for the less potent inhibitors. A control reaction consisted of 0.1% DMSO in place of CFZ and BTZ. Assays were performed at room temperature for 2 h, with readings recorded at 2-min intervals. The maximum velocity over eight sequential readings was calculated and reported as relative fluorescent units per sec (RFU/s). Activity was normalized to the control reaction (0.1% DMSO) and concentration-response curves were generated using GraphPad Prism (version 10.0.0) with a four parameter logistic curve fitting.

2.4 | Proteasome MSP-MS

MSP-MS was performed with a library of 228 synthetic tetradecapeptides that were designed to contain all neighbor and near-neighbor cleavage sites (Lapek et al. 2019; O'Donoghue et al. 2012). Sm20S was first incubated with 500 nM BTZ, CFZ, or 0.1% DMSO (vehicle control). Assays were conducted in quadruplicate by incubating Sm20S with the peptide library at a final concentration of 0.5 μ M for each peptide in 50 mM Tris-HCl, pH 7.5. Assays were incubated at 25°C for 15, 60, and 240 min. At each time point, 20 μ L of the reaction mixture was removed and quenched by the addition of 80 μ L 8M GuHCl. Samples were immediately stored at -80°C. Control reactions consisted of Sm20S pre-incubated with GuHCl to inactivate the enzyme prior to the addition of the peptide library. All samples were desalted using custom-made C18 spin tips and dried in a vacuum centrifuge.

Samples were resuspended in 40 μ L 0.1% formic acid, and ~0.4 μ g peptides were injected into a Q-Exactive Mass Spectrometer equipped with an Ultimate 3000 HPLC (Thermo). Peptides were separated by reverse phase chromatography on a C18 column (1.7 μ m bead size; 75 μ m \times 25 cm; 65°C) at a flow rate of 300 nL min⁻¹ using a 60-min linear gradient of 5%–30% solvent B (0.1% formic acid in acetonitrile), with solvent A being 0.1% formic acid in water. Survey scans were recorded over a 150–2000 *m/z* range (70,000 resolutions at 200 *m/z*, AGC target 3×10^6 , 100 ms maximum). MS/MS was performed in a data-dependent acquisition mode with HCD fragmentation (28 normalized collision energy) on the 12 most intense precursor ions (17,500 resolutions at 200 *m/z*, AGC target 1×10^5 , 50 ms maximum, dynamic exclusion 20 s). Data were processed using PEAKS 8.5 (Bioinformatics Solutions, Inc.). MS² data were searched against the tetradecapeptide library sequences with decoy sequences in reverse order. A precursor tolerance of 20 ppm and 0.01 Da for MS² fragments were defined. No protease digestion was specified. Data were filtered

to a 1% peptide level false discovery rate with the target-decoy strategy. Peptides were quantified with label-free quantification, and data were normalized by median and then filtered by 0.3 peptide quality. Missing and zero values were imputed with random normally distributed numbers in the range of the average of the smallest 5% of the data \pm SD. All mass spectrometry data generated in this study can be accessed on the MASSive repository at this link: <ftp://massive.ucsd.edu/v07/MSV000096255/>.

Cleaved peptides were identified in each dataset as having an 8-fold ($q < 0.05$) or more increase in intensity between 0 and 3 h of incubation. Only cleavage sites located between the 4th and 13th amino acids in the 14-mer peptides were considered. The P4 to P4' amino acids were inputted into the iceLogo software (Colaert et al. 2009) and compared to all possible P4 to P4' sequences in the library. IceLogo plots were generated to illustrate the frequency of amino acids present around the cleavage site.

2.5 | Proteasome activity and inhibition assays

Subunit-specific fluorogenic substrates were custom synthesized and purified by HPLC to >95% by GenScript (New Jersey). Substrates contained either an N-terminal acetylation group and a C-terminal amc group, or an N-terminal 7-methoxycoumarin (mca) and a C-terminal lysine 2,4-dinitrophenyl (K(dnp)). Fluorogenic activity assays were performed in black, round-bottomed 96-well plates. Protein extracts from *Schistosoma* sp. were incubated with inhibitors for 1 h at room temperature, and activity was assayed in a 50- μ L total volume containing 7.5 μ g of protein and 25 μ M Suc-LLVY-amc in 20 mM Tris-HCl, 10 μ M E-64, 0.02% SDS, pH 7.5. For purified Sm20S assays, 10 nM of the enzyme was incubated with a 2-fold serial dilution of the substrate. Controls contained 0.0001% DMSO. Fluorescence was monitored at 24°C in a Synergy HTX multi-mode reader (BioTek Instruments, Winooski, VT). Excitation and emission wavelengths for the amc and mca substrates were 360 and 460 nm, and 320 and 400 nm, respectively. Protease activity was quantified as RFU min⁻¹ μ g⁻¹ protein and normalized to DMSO control reactions.

2.6 | Detection of 20S proteasome activity in three *Schistosoma* species using a fluorescent probe

Schistosoma mansoni, *S. haematobium* and *S. japonicum* protein extracts were subjected to two ammonium sulfate precipitation steps on ice at 30% and 60% saturation for 60 min. The proteasome-containing fractions were

concentrated and buffer exchanged into 100 mM Tris-HCl, 50 μ M E-64, 2 mM AEBSF, 2 μ M pepstatin, pH 7.5, using a 100 kDa centrifugal filter unit (Amicon). Protein was quantified using the bicinchoninic acid assay, and 2.5 and 5 μ g protein were incubated with 2 μ M of the activity-based probe, Me4BodipyFL-Ahx3Leu3VS (R&D Systems, #I-190) (Berkers et al. 2007) at 37°C for 3 h. Samples were mixed with 4X NuPage lithium dodecyl sulfate loading buffer (Invitrogen), heated to 90°C for 5 min, and then loaded onto 12% NuPAGE Bis-Tris Gels (Invitrogen). Proteins were separated using NuPAGE MOPS (3-(*N*-morpholino)propanesulfonic acid) as the running buffer. Twenty nanomolar of human constitutive 20S proteasome (c20S) was used as a positive control. Direct in-gel visualization of Me4BodipyFL-Ahx3Leu3VS-labeled proteasome subunits was performed using a ChemiDoc MP fluorescence scanner (Biorad) with a 530 nm emission filter.

2.7 | Proteasome activity and inhibition assays in three *Schistosoma* species

Extracts of *S. haematobium* (0.625 μ g μ L⁻¹), or *S. japonicum* and *S. mansoni* (each 1.25 μ g μ L⁻¹) were enriched for proteasome by ammonium sulfate precipitation and pre-incubated for 1 h with 500 nM BTZ, CFZ, MZB, or the carmaphycin B analog, CP-17. DMSO (0.125%) was used as a vehicle control. Proteolytic activity was quantified following the addition of an equal volume of 20 μ M mca-VDQMDGW-K(dnp)-NH₂ (β 1-substrate), mca-FnKRR-K(dnp)-NH₂ (β 2-substrate), or 40 μ M Ac-FNKL-amc (β 5-substrate). Assays were performed in 100 mM Tris-HCl, 50 μ M E-64, 1 mM AEBSF, 2 μ M pepstatin, 0.03% SDS, pH 7.5, in a total volume of 8 μ L in a 384-well plate (Greiner Bio-One #784900). The release of the fluorophore was recorded at 24°C in a Synergy HTX plate reader with excitation/emission set to 360/460 nm for the β 5 substrate, and 320/400 nm for the β 1 and β 2 substrates. Experiments were performed in triplicate wells, and DMSO was used as a vehicle control.

2.8 | Protein and structure alignment

Protein sequences were obtained from UniProt that included P28072 (human β 1), G4V926 (*S. mansoni* β 1), C1L5H5 (*S. japonicum* β 1), A0A922LVA0 (*S. haematobium* β 1), Q99436 (human β 2), G4VSW3 (*S. mansoni* β 2), Q5DEZ9 (*S. japonicum* β 2), A0A922LT82 (*S. haematobium* β 2), P28074 (human β 5), A0A5K4F079 (*S. mansoni* β 5), Q5DHC0 (*S. japonicum* β 5), and A0A094ZZD4 (*S. haematobium* β 5). Sequence alignments were performed using MUSCLE (Madeira et al. 2024), and the results were visualized with Jalview (Waterhouse et al. 2009). A structural analysis of the active site was performed using human

proteasome structures available in the Protein Data Bank and the *Schistosoma* proteasome structures predicted by AlphaFold and available on UniProt. For the analysis of the human $\beta 1$ and $\beta 5$ sites, the PDB ID: 6RGQ (Toste Rêgo and da Fonseca 2019) structure was used, while PDB ID: 4R3O (Harshbarger et al. 2015) was used for the $\beta 2$ site as 6RGQ lacked the complete side-chain structure of certain residues. The $\beta 1$ and $\beta 2$ subunit structures of *S. haematobium* were unavailable on UniProt; therefore, these proteins were modeled using ColabFold (Mirdita et al. 2022) (v1.5.5) with default parameters in a Google Colab notebook.

3 | RESULTS

3.1 | Revealing the substrate specificities of the Sm20S β catalytic subunits

We previously isolated Sm20S and identified inhibitors that target the catalytic $\beta 2$ and $\beta 5$ subunits (Bibo-Verdugo et al. 2019). To generate those data, we repurposed three human proteasome substrates, Z-LLE-amc, Boc-LRR-amc, and Suc-LLVY-amc, that had been designed to detect the activity of the c20S $\beta 1$, $\beta 2$, and $\beta 5$ subunits, respectively. Based on the sequence similarity of the c20S $\beta 1$, $\beta 2$, and $\beta 5$ subunits with their equivalent subunits in Sm20S, we predicted that each of the three classical c20S subunit-specific substrates would also be cleaved by the respective β subunits of Sm20S. However, when comparing the turnover rate of these substrates by c20S and Sm20S, it was evident that they were more efficiently cleaved by c20S (Bibo-Verdugo et al. 2019). This encouraged us to develop Sm20S subunit-specific substrates that would be cleaved with higher efficiencies and serve as valuable tools to screen for new inhibitors of Sm20S, to uncover the importance of each catalytic subunit for the growth and survival of *S. mansoni* and to provide a starting point for rational inhibitor design. Accordingly, we utilized MSP-MS to define the cleavage specificities of each of the three catalytic β subunits.

We have previously shown that c20S, the human 20S immunoproteasome (i20S), and Pf20S each cleave at more than 200 sites within the MSP-MS peptide library (Li et al. 2016; Winter et al. 2017). In this study, we chromatographically isolated Sm20S and incubated it with the same peptide library for 1 and 3 h, which resulted in the detection of 164 sites and 252 cleavage sites, respectively. The frequency of each amino acid found in the P4 to P4' sites surrounding the cleavage site was evaluated using iceLogo, which revealed that Sm20S has a strong preference for cleavage of peptides with Lys in the P2 position, Arg in P3,

P1' and P2', and Trp in P4 (Figure S1, Supporting Information).

It is not clear which of the three catalytic β subunits was responsible for cleaving each of these peptides, and their physical separation is not possible without inactivation of the whole complex. Accordingly, we used inhibitors to selectively inactivate one or more of the Sm20S catalytic β subunits such that the activity of the remaining non-inhibited subunits could be measured. To do this, we generated a concentration-response curve with CFZ and determined that it inhibits the $\beta 5$ subunit more potently than either $\beta 1$ or $\beta 2$. In the presence of 500 nM CFZ, the $\beta 5$ subunit activity measured using Suc-LLVY-amc was strongly inhibited, whereas the activities of $\beta 1$ (Z-LLE-amc) and $\beta 2$ (Boc-LRR-amc) were only reduced by ~40% (Figure 1b). Therefore, 500 nM CFZ was used for follow-up MSP-MS studies to distinguish $\beta 5$ activity from $\beta 1$ and $\beta 2$.

Next, we performed a concentration-response study with BTZ and showed that the $\beta 5$ and $\beta 1$ subunits were preferentially inhibited over $\beta 2$. Using 500 nM BTZ, $\beta 5$ and $\beta 1$ are strongly inhibited, whereas $\beta 2$ activity was reduced by only ~35% (Figure 1c). Thus, the data reveal that BTZ distinguishes $\beta 1$ and $\beta 5$ activities from $\beta 2$. The cleavage specificity of $\beta 1$ can then be determined as enzyme activity that is preferentially inhibited by BTZ relative to CFZ, whereas the $\beta 2$ activity is weakly inhibited by both. By understanding the inhibitor conditions needed to isolate one or the other β catalytic activity, we then performed MSP-MS in the presence of either 500 nM CFZ or BTZ to determine which subunit was responsible for cleaving which peptides.

3.2 | Development of a Sm20S $\beta 5$ substrate

MSP-MS cleavage products generated in the absence (DMSO) and presence of CFZ were compared. The intensity of 64 of those cleavage products was reduced by 2.5-fold or more in the presence of CFZ (Data S1). Two example peptides that show this pattern are GQYPnFVKI*STTHW and HHFTQRAGILKL*nP wherein cleavage occurs at the site marked with an asterisk. In these peptides, the lowercase n corresponds to norleucine, an isostere of methionine. The N-terminal cleavage products (highlighted in bold in Figure 2a,b) increased with time in the uninhibited reaction (0.1% DMSO) but did not increase in the presence of CFZ. BTZ also reduced cleavage of these sites, albeit with lower potency than CFZ. We generated a substrate specificity profile of the amino acids in the P4 to P4' positions of these 64 cleavage sites and found a preference for hydrophobic amino acids at P4 and P1, N, H, and W at P3, and K and T at P2 (Figure 2c). On the prime side, A, R, K, and N were most frequently found at P1' while W, F, and P were found at P2', P3',

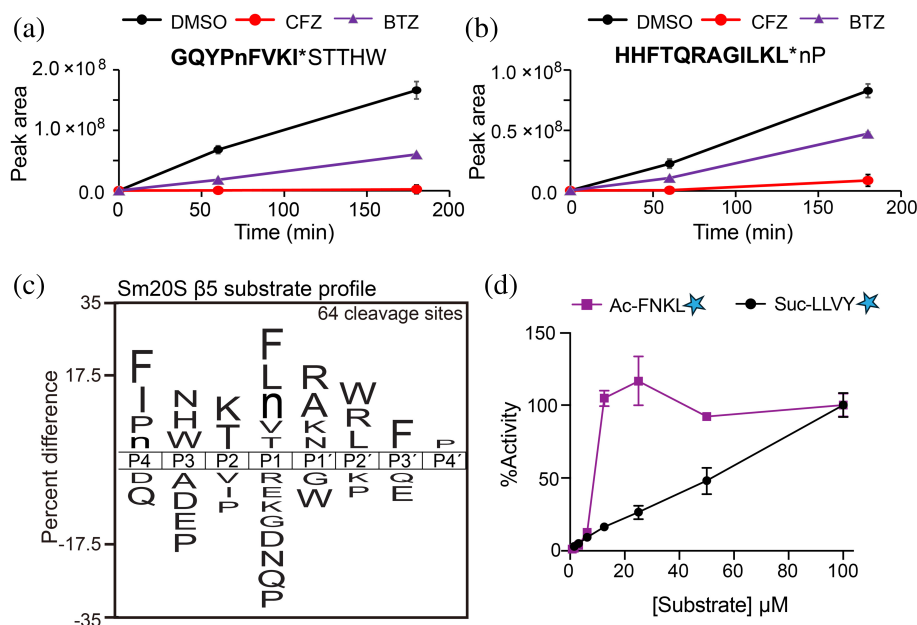


FIGURE 2 MSP-MS profiling of the Sm20S β5 catalytic subunit. (a) An example of one peptide (out of 42) that is cleaved by Sm20S in the MSP-MS assay. The N-terminal cleaved product (bolded) increases with time in the presence of vehicle (DMSO) but is reduced by the presence of 500 nM CFZ or 500 nM BTZ. (b) Another example peptide that is cleaved with lower efficiency in the presence of CFZ and BTZ. (c) IceLogo plot illustrating the P4 to P4' substrate profile of Sm20S β5. (d) Comparison of the hydrolysis of the newly synthesized substrate, Ac-FNKL-amc, compared to the traditional c20S β5 substrate, Suc-LLVY-amc, as a function of concentration. Data were normalized as relative activity using 100 μM of each substrate. The light blue star represents the amc fluorophore. Mass spectrometry-based assays were performed in technical quadruplicate whereas fluorogenic substrate assays were performed in technical triplicate.

and P4', respectively. Using this information, we synthesized the substrate, Ac-FNKL-amc, which contains several amino acids that are favored by Sm20S β5 in the P4 to P1 positions and compared its hydrolysis to that of the c20S substrate, Suc-LLVY-amc. At increasing concentrations, we show that cleavage of Ac-FNKL-amc is maximal at 25 μM and occurs at a ~4-fold higher rate than with Suc-LLVY-amc at the same concentration (Figure 2d).

3.3 | Development of a Sm20S β1 substrate

We next evaluated the MSP-MS cleavage products that were strongly inhibited by 500 nM BTZ relative to 500 nM CFZ, that is, isolating for β1 activity. We found 11 cleavage products that matched this profile. Example peptides that are cleaved under these conditions include TEIWE*PIDRGPWRF (Figure 3a) and KHPLETVYAD*SSEW (Figure 3b), whereby the cleavage products increase over time in the presence of vehicle (0.1% DMSO), but this product formation is reduced in the presence of BTZ and less so with CFZ. Many of these peptides had either Glu or Asp in the P1 position, a finding that is common for the β1 subunit of other proteasomes (Fajtova et al. 2024; Kisselev et al. 2003). We attempted to synthesize several tetrapeptide-amc substrates but had low yield and

purity due to inefficient coupling of Glu and Asp to the amc group. Therefore, we searched for commercially available protease substrates containing E or D that could be cleaved by Sm20S β1. We found that the caspase-3 substrate, mca-VDQMD*GW-K(dnp) was hydrolyzed by Sm20S. Importantly, this activity was inhibited by 100 nM BTZ but not by 100 nM CFZ, which is similar to the inhibition profile generated when using the human c20S β1 subunit, LLE-amc (Figure 3d). When both substrates were evaluated over a concentration range of 2–500 μM, VDQMD*GW was cleaved with a ~2-fold greater efficiency between 16 and 250 μM (Figure 3e).

3.4 | Development of a Sm20S β2 substrate

We next evaluated the MSP-MS peptide cleavage profiles that were neither inhibited by BTZ nor CFZ at 500 nM, that is, primarily due to the activity of the β2 subunit. We found 137 cleaved peptides that fit this criterion, exemplified by YQLLTnNEIFR*KWH and HWAFRSR*YHGPLAH (Figure 4a,b). The overall profile indicated a high frequency of cleavage when R is present at P3, P1, and P1', and K is present at P2 (Figure 4b). Importantly, we show that L and D were not favored in the P1 position by the β2 subunit, which supported our choice of using these amino acids in the

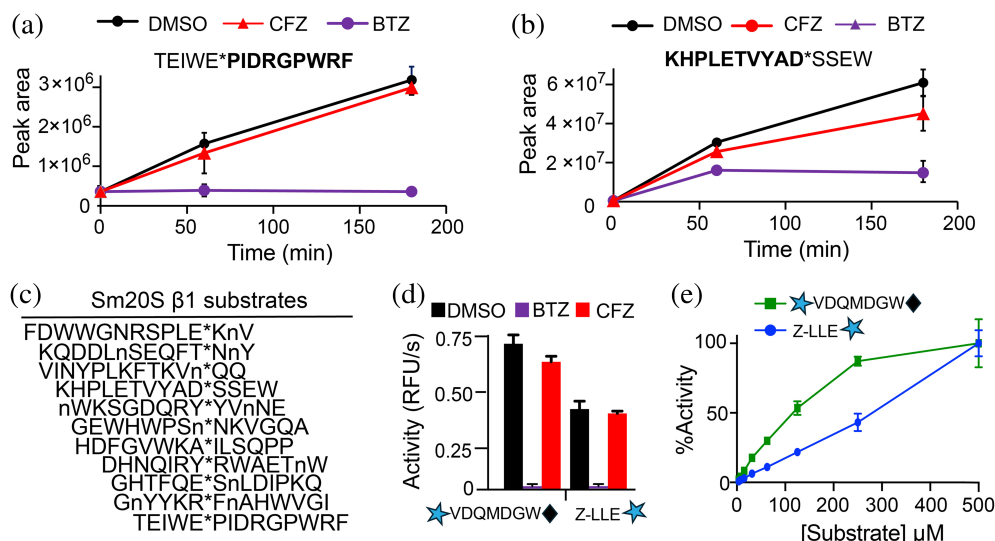


FIGURE 3 MSP-MS profiling of the Sm20S β1 catalytic subunit. (a) An example of a peptide cleaved by Sm20S in the MSP-MS assay showing the formation of the cleavage product is reduced by 500 nM BTZ. The peak area for the C-terminal cleavage product (bolded) is being measured. (b) Another example of a cleavage product from the MSP-MS assay that is decreased in abundance in the presence of 500 nM BTZ. The N-terminal cleavage product (bolded) is being measured. (c) List of Sm20S β2 substrates. Their cleaved products are preferentially reduced by BTZ. (d) Activity of Sm20S in the presence of 500 nM BTZ and CFZ using 10 μM of caspase 3 substrate (mca-VDQMDGW-K(dnp)) and 10 μM of the c20S β1-specific substrate, Z-LLE-amc. (e) Comparison of the hydrolysis of mca-VDQMDGW-K(dnp) and LLE-amc by Sm20S as a function of concentration. Data were normalized as relative activity using 500 μM of each substrate. The light blue star represents the amc fluorophore. The light blue star represents the amc fluorophore and the black diamond represents the K(dnp) quencher. Mass spectrometry-based assays were performed in technical quadruplicates, and fluorogenic substrate assays were performed in technical triplicates.

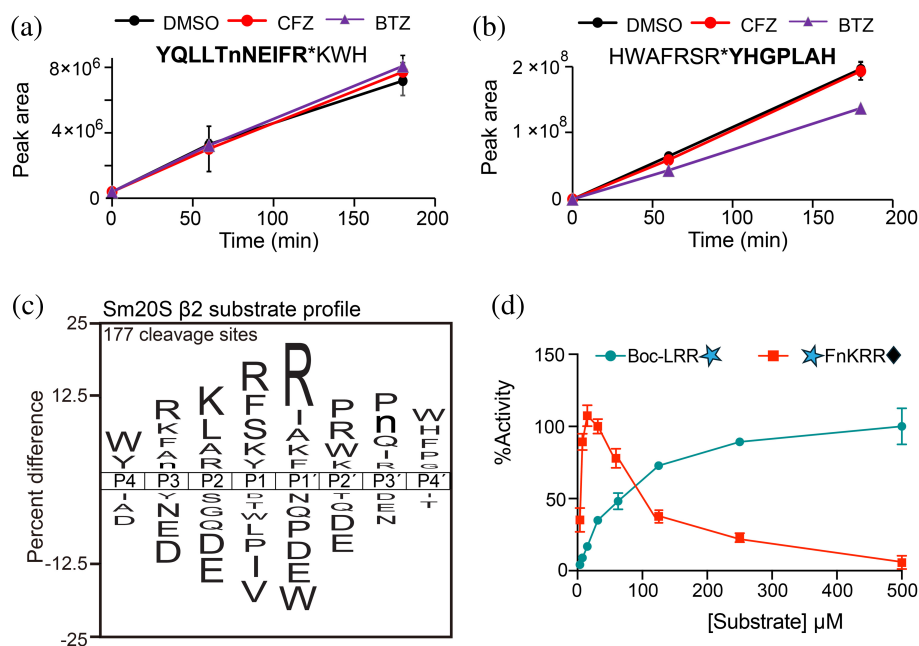


FIGURE 4 MSP-MS profiling of the Sm20S β2 catalytic subunit. (a) An example of a peptide cleaved by Sm20S, peptides highlighted in bold, in the presence of 500 nM of both BTZ and CFZ when compared to vehicle control (DMSO). The cleavage product (bolded) increases at the same rate in the presence or absence of inhibitor. (b) Another example cleavage product (bolded) for which formation is unaffected by the presence of inhibitors. (c) iceLogo plot illustrating the substrate profile of 177 peptide substrates that are cleaved by Sm20S. (d) Comparison of the hydrolysis of the fluorescent mca-FmKRR-K(dnp) and the c20S β2-specific substrate, Boc-LRR-amc, as a function of concentration. Data were normalized as relative activity using 500 μM of Boc-LRR-amc and 31.25 μM of mca-FmKRR-K(dnp). The light blue star represents the amc fluorophore and the black diamond represents the K(dnp) quencher. Mass spectrometry-based assays were performed in technical quadruplicate whereas fluorogenic substrate assays were performed in technical triplicate.

P1 position for the $\beta 5$ and $\beta 1$ subunits, respectively. As R in P1' is the most frequently found amino acid across all eight positions (P4 to P4'), we decided to include this amino acid in the substrate design. Therefore, we made an internally quenched substrate consisting of the sequence mca-FnKRR-K(dnp) in which cleavage occurs between the two R residues. Cleavage of mca-FnKRR-K(dnp) and Boc-LRR-amc was then evaluated over a concentration range of 6.25–500 μ M. For reasons yet unclear, Sm20S cleaved mca-FnKRR-K(dnp) with high efficiency up to 50 μ M, after which a reduction in activity was measured up to 500 μ M. By contrast, cleavage of Boc-LRR-amc steadily increased across the entire concentration range tested (Figure 4c).

3.5 | Testing new substrates with single-step enriched Sm20S from cell extracts

The isolation of Sm20S to homogeneity is labor-intensive and costly due to the need for vertebrate animals to produce sufficient *S. mansoni* worms. Therefore, using our three new β subunit-specific substrates, we evaluated Sm20S activity in a *S. mansoni* protein extract subjected to only ammonium sulfate precipitation (30% and 60% saturation), the first step of the

three-step purification process. Pepstatin, E-64, and AEBSF were included in the assay buffer to prevent substrate cleavage by *S. mansoni* aspartyl, cysteine, and serine proteases (Caffrey et al. 2004; Caffrey and Ruppel 1997; Horn et al. 2014), respectively, in the single-step enriched Sm20S. Our analysis of the enriched Sm20S extract revealed detectable $\beta 1$, $\beta 2$, and $\beta 5$ peptidase activities. Notably, the reaction velocities (RFU/s) that were quantified using the new substrates were at least 9-fold greater than the old substrates (Figure 5a–c). Furthermore, we compared the inhibition profiles of the enriched extract to that of the purified enzyme, demonstrating a consistent inhibition pattern with 10 μ M bortezomib (BTZ) and 10 μ M carfilzomib (CFZ) (Figure 5d). These studies confirm that using the new substrates, the single-step-enriched Sm20S is sufficient to specifically measure the $\beta 1$, $\beta 2$, and $\beta 5$ activities.

We next determined whether the potency of BTZ and CFZ could be directly measured in the single-step-enriched Sm20S. BTZ was found to have an IC_{50} value of 49.84 ± 0.24 nM for the Sm20S $\beta 1$ subunit and 17.97 ± 2.05 nM for the $\beta 5$ subunit (Figure 5e). No reduction of $\beta 2$ activity was detected up to 5 μ M. CFZ displayed an IC_{50} of 2.50 ± 0.51 nM for $\beta 5$ and 288.0 ± 90 nM for Sm20S $\beta 2$ (Figure 5f). The $\beta 1$ subunit was

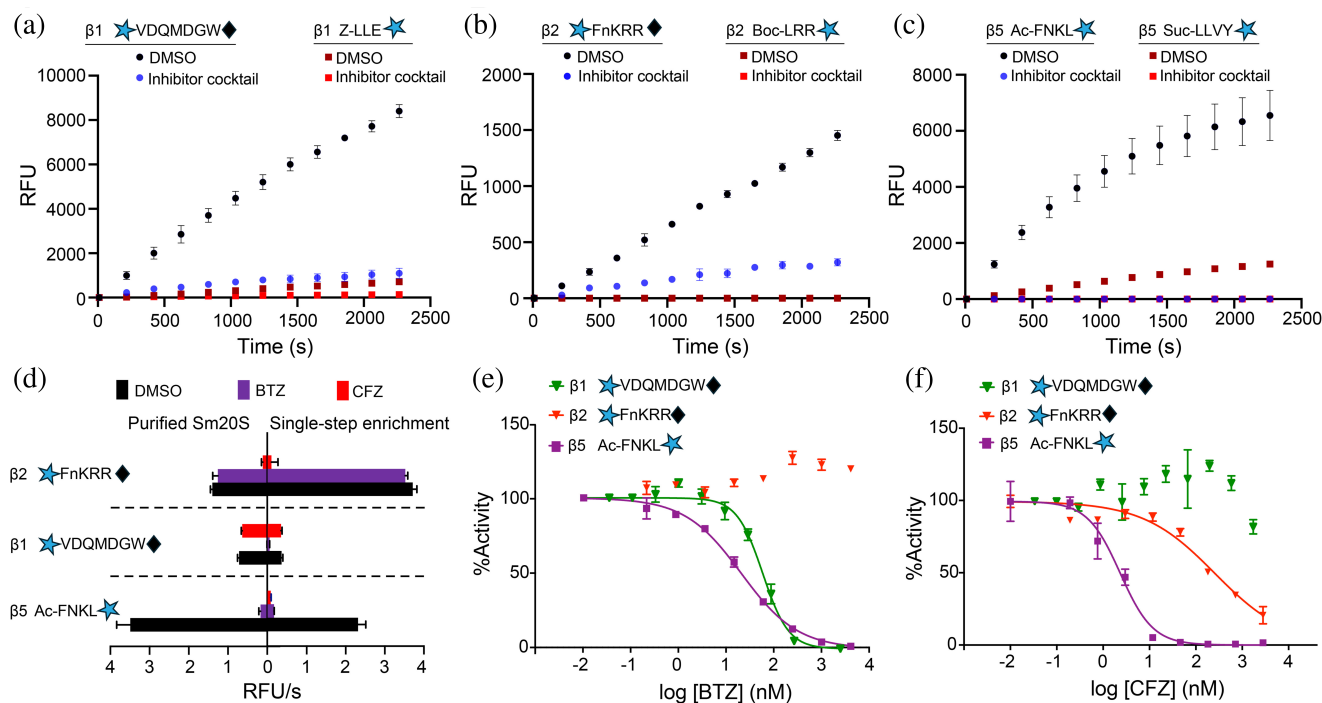


FIGURE 5 Evaluation of Sm20S substrates with pure Sm20S and single-step enriched Sm20S. (a–c) Proteolytic activity of single-step enriched Sm20S over time using the newly synthesized and classic substrates in the absence (DMSO) or presence of a proteasome inhibitor cocktail (10 μ M each of BTZ, CFZ and MZB). The light blue star represents the amc fluorophore and the black diamond represents the K(dnp) quencher. (d) Comparison of the activities of purified Sm20S and the single-step enriched Sm20S using 10 μ M of the newly developed substrates. Assays were performed in the presence of 500 nM of BTZ or CFZ. (e) Dose–response curves for each catalytic subunit of Sm20S (single-step enriched) in the presence of BTZ. (f) Dose–response curves for each catalytic subunit of Sm20S (single-step enriched) in the presence of CFZ. Data are shown as means \pm SD of technical triplicates. Curve fittings were generated using GraphPad Prism, but fittings could not be made for $\beta 2$ activity in (e) and $\beta 1$ activity in (f).

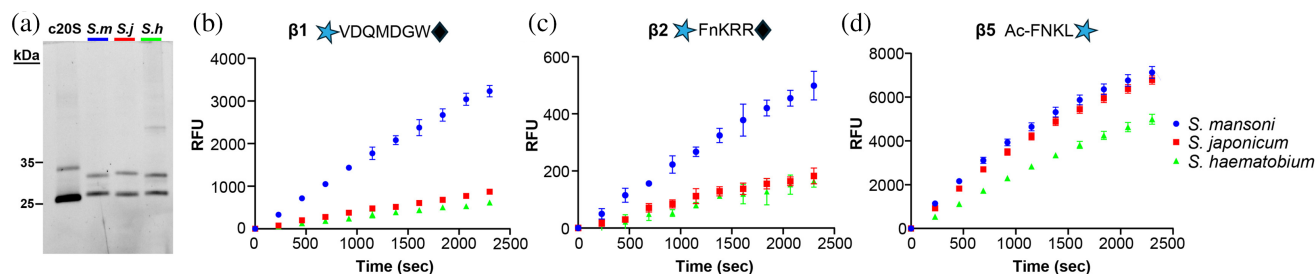


FIGURE 6 Comparison of the 20S activities from three *Schistosoma* species with the subunit-specific substrates. (a) Visualization of *Schistosoma* spp. proteasome activity using the fluorescent Me4BodipyFL-Ahx3Leu3VS activity-based probe. This probe was used to normalize the activity of the single-step enriched proteasomes in advance of the fluorogenic substrate assays (panels (b)–(d)). Approximately 2.5 μ g *S. haematobium* lysate, and 5 μ g *S. japonicum* and *S. mansoni* lysates were loaded into each lane, and c20S was used as a control. (b) Cleavage of VDQMD*GW by the schistosome β 1 subunit. (c) Cleavage of FnkRR*K by the schistosome β 2 subunit. (d) Cleavage of FNKL*K by the schistosome β 5 subunit. Data for fluorescent assays are shown as means \pm SD of technical triplicates.

inhibited by 15% at 5 μ M. These data demonstrate that dose–response assays can be performed using proteasome inhibitors and the single-step enriched Sm20S. A comparison of the BTZ and CFZ dose–response curves, utilizing both the old and new substrates, reveals significant differences in subunit specificity. Specifically, 10 μ M BTZ completely inhibited β 2 activity with the old substrate, Boc-LRR-amc (Figure 1c). However, at the same concentration, BTZ did not inhibit β 2 activity when using the new substrate, mca-FnkRR-K (dnp) (Figure 5e). This discrepancy suggests that Boc-LRR-amc is not exclusively cleaved by β 2 and is processed by the β 5 and/or β 1 subunits. Similarly, 10 μ M CFZ fully inhibited β 1 activity with the old substrate, Z-LLE-amc (Figure 1b), but is only partially inhibitory with the new substrate, mca-VDQMDGW-K(dnp) (Figure 5f). This suggests that Z-LLE-amc is also susceptible to cleavage by β 5 and/or β 2. In summary, these observations demonstrate that the new substrates not only exhibit higher cleavage efficiency but also provide improved subunit specificity compared to the older substrates.

3.6 | The subunit specificity of the 20S proteasome from three *Schistosoma* species

The new β 1, β 2, and β 5 substrates were designed based on the specificity profile of the 20S from *S. mansoni*, which is the laboratory model. New anti-schistosomal drugs should be active against *S. mansoni* and the other two medically important schistosomes, *S. haematobium* and *S. japonicum* (Caffrey 2007; Caldwell et al. 2023). Thus, it is relevant to understand whether the substrates developed for Sm20S can also be used for the other two species. We first normalized proteasome amounts in extracts of all three schistosome species using the proteasome activity-based probe, Me4BodipyFL-Ahx3Leu3VS (Verdoes et al. 2006). This probe labeled three subunits of human c20S, with the bottom two bands co-migrating

to yield one strongly fluorescent product (Figure 6a). The probe labeled two of the three β subunits in each of the schistosome extracts.

Once the proteasome amounts had been normalized, we evaluated the catalytic β subunit activities with the subunit-specific substrates. The specific activity using the β 1 and β 2 substrates was two- to three times higher for *S. mansoni* than for *S. haematobium* and *S. japonicum* (Figure 6b–d), whereas the activities measured using the β 5 substrate were similar for the three species. It is unclear why substrate cleavage activity is lower for the β 1 and β 2 subunits of *S. japonicum* 20S proteasome (Sj20S) and *S. haematobium* 20S proteasome (Sh20S) considering that Sm20S has more than 94% sequence identity with Sj20S and Sh20S across all three catalytic subunits. For the β 1 subunit specifically, Sm20S is 96% and 99% identical to Sj20S and Sh20S, respectively, whereas for the β 2 subunit, Sm20S is 94% and 98% identical to Sj20S and Sh20S, respectively (Figure S2). In a structural overlay of the residues adjacent to the catalytic Thr, the β 1 and β 5 subunits are 100% identical, while the β 2 site has a different residue in position 24 for each of the three species (Sm20S–Thr₂₄, Sj20S–Asn₂₄, and Sh20S–Ser₂₄). Differences in the rate of substrate cleavage might, therefore, be due to other factors such as substrate access to the inner core of the proteasome which is controlled by several regulatory proteins in the 19S cap. Overall, the data reveal that the new substrates work well with the proteasomes of all three medically important schistosomes and can be used in the future for inhibition assays of the respective β catalytic subunits.

Schistosome extracts were then pre-incubated with 500 nM BTZ or CFZ to test their cross-species inhibitory effects. Similar inhibition profiles were recorded for the three species (Figure 7a–c). BTZ preferentially inhibited β 1 and β 5, whereas CFZ inhibited β 5 and β 2 more than β 1. In addition, we tested MZB, a pan-catalytic β subunit inhibitor that is in Phase 3 clinical trials for the treatment of glioblastoma (Roth et al. 2024). MZB (250 nM) decreased the activity measured with

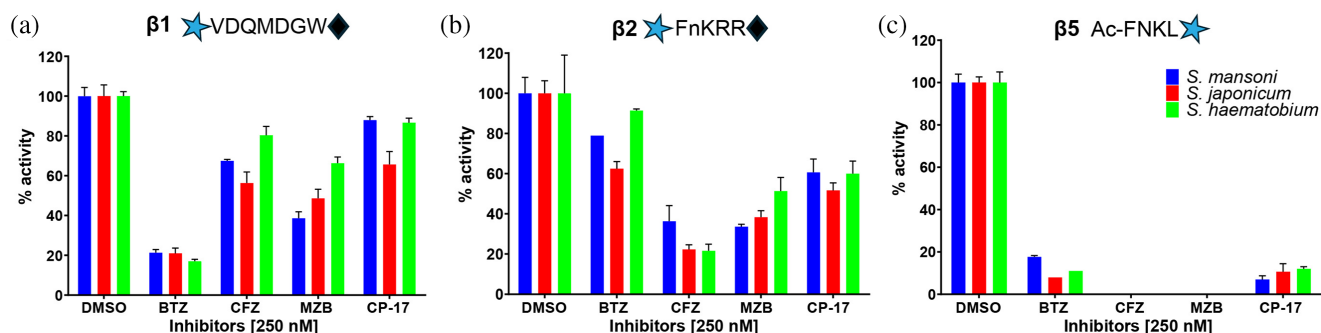


FIGURE 7 Comparison of proteasome inhibition across three *Schistosoma* species by cleavage of the fluorescent subunit-specific substrates. Proteasome inhibitors were pre-incubated for 1 h with single-step enriched 20S enzymes from the three *Schistosoma* species. Activity was then assayed with the (a) $\beta 1$ -, (b) $\beta 2$ - and (c) $\beta 5$ -specific substrates. Data are shown as means \pm SD of technical triplicates.

each of the three substrates; specifically, a complete inactivation of $\beta 5$, a 66 to 48% decrease in $\beta 2$ activity, and a 61 to 34% reduction in $\beta 1$ activity. Finally, our previous studies revealed that the proteasome inhibitor CP-17, an analog of the marine natural product, carmaphycin B, demonstrated potent anti-schistosomal activity (Bibo-Verdugo et al. 2019). Using the subunit-specific substrates, we evaluated the potency of CP-17 at 250 nM and determined that it preferentially targets $\beta 5$ (>90% reduction) over $\beta 2$ (44–48% reduction) with little inhibition of $\beta 1$ being observed. These data are consistent with our previous studies using the purified enzyme (Bibo-Verdugo et al. 2019).

The similar inhibition responses observed across the three *Schistosoma* species for each catalytic β subunit suggest that proteasome inhibitors developed against one species will likely be effective against the other two. This discovery will significantly streamline the drug development process by reducing the need for extensive testing across all three species.

4 | DISCUSSION

The reliance on praziquantel to treat schistosomiasis and the associated concerns regarding potential resistance, coupled with the drug's pharmaceutical and pharmacological limitations, encourage the exploration of alternative chemotherapeutics. Therefore, we focused on the 20S proteasome of the schistosome, given the preclinical and clinical success of targeting the orthologous protein in both *Plasmodium* and *Leishmania* (Liu et al. 2024b).

The 20S proteasome is a large multi-subunit, ATP-dependent proteolytic complex that regulates several cellular processes, including normal protein turnover and degradation of misfolded proteins. Inhibitors of c20S, for example, CFZ and BTZ, are key drugs for the treatment of blood cancers, and more recently, zeto-mipzomib (KZR-616) is one of several new inhibitors of i20S that are in clinical trials for the treatment of autoimmune diseases and immune-mediated disorders (Kirk et al. 2021). Importantly, anti-cancer proteasome

inhibitors targeting Sm20S kill *S. mansoni* in vitro (Bibo-Verdugo et al. 2017). Also, inhibition of 19S proteasome deubiquitinating activity in the parasite induces a modest reduction in egg production in vitro, decreases viability, and is eventually lethal (do Patrocinio et al. 2020). Taken together, these data suggest that the schistosome proteasome is a drug target of interest for the potential treatment of schistosomiasis and encourage the characterization of the cleavage specificities of the individual 20S catalytic β subunits, information that would underpin a campaign to develop *Schistosoma*-selective proteasome inhibitors.

In eukaryotes, each of the 20S catalytic subunits has a distinct substrate specificity that varies between organisms (Maurits et al. 2020). Fluorogenic substrates such as Z-LLE-amc, Boc-LRR-amc, and Suc-LLVY-amc, which were developed for the $\beta 1$, $\beta 2$, and $\beta 5$ subunits of c20S, respectively, are also cleaved by the respective subunits of parasite proteasomes (Li et al. 2014; Wyllie et al. 2019). However, using MSP-MS-directed substrate design, we show that these c20S substrates are not optimal for Sm20S $\beta 1$, $\beta 2$, and $\beta 5$, and that we could optimize a new substrate for each β subunit that performed 2- to 8-fold better. These rationally optimized β subunit-selective substrates for Sm20S, therefore, should prove valuable in the design of inhibitors targeting each β subunit or combinations of β subunits. As a case in point, our MSP-MS studies suggest that the preferential cleavage of the sequence RKR*R (where * is the cleavage site) by Sm20S $\beta 2$ (Figure 3b) is different from the cleavage preference of the c20S $\beta 2$ subunit for which positively charged residues at P2 are not favored. For the $\beta 5$ subunit, Sm20S prefers Thr at P2 and Asn at P3, both of which are not well tolerated by c20S at the same positions (Rut et al. 2018). Accordingly, our future inhibitor design efforts will focus on exploiting these differences to develop potent inhibitors of Sm20S that bind weakly to the host proteasome and, therefore, decrease cytotoxicity to mammalian cells.

We also developed a single-step enrichment of Sm20S activity from crude extracts using ammonium sulfate, which, when combined with the new specific substrates, allowed for a more streamlined evaluation

of inhibitor engagement without the need for isolating pure Sm20S, a time-consuming process that would require the use of more vertebrate host animals. It was evident that the catalytic activity of $\beta 1$ and $\beta 2$ is higher for Sm20S than for Sj20S and Sh20S even though the protein sequences are >94% identical. It is possible that the 19S regulatory subunits that interact with each 20S proteasome may play a role in regulating substrate entry to the inner chamber of the proteasome and thus modulate catalytic activity with the new substrates.

Encouragingly, similar inhibition profiles were observed for the 20S proteasomes of *S. mansoni*, *S. haematobium* and *S. japonicum*, using both anti-cancer inhibitors and a carmaphycin B analog. This suggests that inhibitors that engage the 20S in *S. mansoni*, the most experimentally tractable species, could be broadly effective against the other two species. This would save time and money and align with the preferred target product profile for schistosomiasis drugs (Caffrey 2007; Caldwell et al. 2023), which calls for drugs that are active against all three major schistosome species.

In conclusion, our study employed mass spectrometry to characterize the substrate specificities of Sm20S $\beta 1$, $\beta 2$, and $\beta 5$, leading to the design of new fluorogenic reporter substrates. These substrates enabled the development of a rapid enrichment method for the schistosome proteasome and revealed conserved inhibitor susceptibilities between the three important *Schistosoma* species. This paves the way for a program to develop broad-spectrum anti-schistosomal inhibitors that focus on the Sm20S proteasome.

AUTHOR CONTRIBUTIONS

Elany B. Silva: Methodology; investigation; writing – review and editing; validation; data curation; formal analysis. **Zhenze Jiang:** Writing – original draft; methodology; conceptualization; investigation; software; visualization; formal analysis. **Chenxi Liu:** Writing – original draft; methodology; investigation; formal analysis. **Pavla Fajtová:** Investigation. **Thaiz R. Teixeira:** Investigation; validation. **Giovana de Castro Fiorini Maia:** Visualization. **Lawrence J. Liu:** Investigation. **Nelly El-Sakkary:** Investigation. **Danielle E. Skinner:** Investigation. **Ali Syed:** Investigation. **Steven C Wang:** Investigation; methodology. **Conor R. Caffrey:** Conceptualization; funding acquisition; project administration; supervision; writing – review and editing; formal analysis; resources. **Anthony J. O'Donoghue:** Conceptualization; funding acquisition; project administration; supervision; visualization; writing – review and editing; data curation; formal analysis; resources.

ACKNOWLEDGMENTS

The research was supported by NIH awards R21AI133393 and R21AI171824 to AJO and CRC, and R01AI158612 and R21AI146387 to AJO. The content is solely the responsibility of the authors and does not

necessarily represent the official views of the National Institutes of Health. PF received funding from the Program for Research and Mobility Support of Starting Researchers from the Czech Academy of Sciences (MSM200551901) and the European Union's Horizon 2020 research and innovation program under the Marie Skłodowska-Curie grant agreement No. 846688, ProTeCT.

DATA AVAILABILITY STATEMENT

The data that support the findings of this study are openly available in MassIVE at <https://massive.ucsd.edu/ProteoSAFe/static/massive.jsp?redirect=auth>, reference number MSV000096255.

ORCID

Anthony J. O'Donoghue  <https://orcid.org/0000-0001-5695-0409>

REFERENCES

- Abdulla M-H, Lim K-C, Sajid M, McKerrow JH, Caffrey CR. *Schistosomiasis mansoni*: novel chemotherapy using a cysteine protease inhibitor. *PLoS Med*. 2007;4:e14.
- Abdulla MH, Ruelas DS, Wolff B, Snedecor J, Lim KC, Xu F, et al. Drug discovery for schistosomiasis: hit and lead compounds identified in a library of known drugs by medium-throughput phenotypic screening. *PLoS Negl Trop Dis*. 2009;3:e478.
- Almaliti J, Fajtová P, Calla J, LaMonte GM, Feng M, Rocamora F, et al. Development of potent and highly selective epoxyketone-based plasmodium proteasome inhibitors. *Chemistry*. 2023;29:e202203958.
- Altun M, Galardy PJ, Shringarpure R, Hideshima T, LeBlanc R, Anderson KC, et al. Effects of PS-341 on the activity and composition of proteasomes in multiple myeloma cells. *Cancer Res*. 2005;65:7896–901.
- Andrews P, Thomas H, Pohlke R, Seubert J. Praziquantel. *Med Res Rev*. 1983;3:147–200.
- Augello G, Modica M, Azzolina A, Puleio R, Cassata G, Emma MR, et al. Preclinical evaluation of antitumor activity of the proteasome inhibitor MLN2238 (ixazomib) in hepatocellular carcinoma cells. *Cell Death Dis*. 2018;9:28.
- Badoco FR, Paula LAL, Orenha RP, Mendes TMF, Squarisi IS, el-Sakkary N, et al. EF24, a schistosomicidal curcumin analog: insights from its synthesis and phenotypic, biochemical and cytotoxic activities. *Chem Biol Interact*. 2022;368:110191.
- Bard JAM, Goodall EA, Greene ER, Jonsson E, Dong KC, Martin A. Structure and function of the 26S proteasome. *Annu Rev Biochem*. 2018;87:697–724.
- Basch PF. Cultivation of *Schistosoma mansoni* in vitro. I. Establishment of cultures from cercariae and development until pairing. *J Parasitol*. 1981;67:179–85.
- Beekman C, Jiang Z, Suzuki BM, Palmer JM, Lindner DL, O'Donoghue AJ, et al. Characterization of PdCP1, a serine carboxypeptidase from *Pseudogymnoascus destructans*, the causal agent of white-nose syndrome. *Biol Chem*. 2018;399:1375–88.
- Bennett JM, Ward KE, Muir RK, Kabeche S, Yoo E, Yeo T, et al. Covalent macrocyclic proteasome inhibitors mitigate resistance in *Plasmodium falciparum*. *ACS Infect Dis*. 2023;9:2036–47.
- Berkers CR, van Leeuwen FWB, Groothuis TA, Peperzak V, van Tilburg EW, Borst J, et al. Profiling proteasome activity in tissue with fluorescent probes. *Mol Pharm*. 2007;4:739–48.
- Bibo-Verdugo B, Jiang Z, Caffrey CR, O'Donoghue AJ. Targeting proteasomes in infectious organisms to combat disease. *FEBS J*. 2017;284:1503–17.

- Bibo-Verdugo B, Wang SC, Almaliti J, Ta AP, Jiang Z, Wong DA, et al. The proteasome as a drug target in the metazoan pathogen, *Schistosoma mansoni*. *ACS Infect Dis*. 2019;5(10):1802–12. <https://doi.org/10.1021/acsinfecdis.9b00237>
- Bota DA, Mason W, Kesari S, Magge R, Winograd B, Elias I, et al. Marizomib alone or in combination with bevacizumab in patients with recurrent glioblastoma: phase I/II clinical trial data. *Neurooncol Adv*. 2021;3:vdab142.
- Caffrey CR. Chemotherapy of schistosomiasis: present and future. *Curr Opin Chem Biol*. 2007;11:433–9.
- Caffrey CR. Schistosomiasis and its treatment. *Future Med Chem*. 2015;7:675–6.
- Caffrey CR, El-Sakkary N, Mäder P, Krieg R, Becker K, Schlitzer M, et al. Drug discovery and development for schistosomiasis. In: Swinney D, Pollastri M, editors. *Neglected tropical diseases: drug discovery and development*. Volume 77. Weinheim, Wiley-VCH; 2019. p. 187–225.
- Caffrey CR, McKerrow JH, Salter JP, Sajid M. Blood “n” guts: an update on schistosome digestive peptidases. *Trends Parasitol*. 2004;20:241–8.
- Caffrey CR, Ruppel A. Cathepsin B-like activity predominates over cathepsin L-like activity in adult *Schistosoma mansoni* and *S. japonicum*. *Parasitol Res*. 1997;83:632–5.
- Caldwell N, Afshar R, Baragaña B, Bustinduy AL, Caffrey CR, Collins JJ, et al. Perspective on schistosomiasis drug discovery: highlights from a schistosomiasis drug discovery workshop at Wellcome collection, London, September 2022. *ACS Infect Dis*. 2023;9:1046–55.
- Chen D, Frezza M, Schmitt S, Kanwar J, Dou PQ. Bortezomib as the first proteasome inhibitor anticancer drug: current status and future perspectives. *Curr Cancer Drug Targets*. 2011;11:239–53.
- Cioli D, Pica-Mattoccia L, Basso A, Guidi A. Schistosomiasis control: praziquantel forever? *Mol Biochem Parasitol*. 2014;195:23–9.
- Colaert N, Helsen K, Martens L, Vandekerckhove J, Gevaert K. Improved visualization of protein consensus sequences by ice-Logo. *Nat Methods*. 2009;6:786–7.
- Colley DG, Bustinduy AL, Secor WE, King CH. Human schistosomiasis. *Lancet*. 2014;383:2253–64.
- Danso-Appiah A, Owiredo D, Asiamah M, Akuffo K, Eusebi P, Jiangang G, et al. Safety of praziquantel in persons with and without schistosomiasis: systematic review and meta-analysis. 2022. Preprint at <https://doi.org/10.1101/2022.03.09.22270839>
- do Patrocinio AB, Cabral FJ, Bitencourt ALB, Brigato OM, Magalhães LG, de Lima Paula LA, et al. Inhibition of 19S proteasome deubiquitinating activity in *Schistosoma mansoni* affects viability, oviposition, and structural changes. *Parasitol Res*. 2020;119(7):2159–76. <https://doi.org/10.1007/s00436-020-06686-4>
- Fajtova P, Hurysz BM, Miyamoto Y, Serafim MSM, Jiang Z, Vazquez JM, et al. Distinct substrate specificities of the three catalytic subunits of the *Trichomonas vaginalis* proteasome. *Protein Sci*. 2024;33:e5225.
- Fukushige M, Chase-Topping M, Woolhouse MEJ, Mutapi F. Efficacy of praziquantel has been maintained over four decades (from 1977 to 2018): a systematic review and meta-analysis of factors influence its efficacy. *PLoS Negl Trop Dis*. 2021;15:e0009189.
- Groen K, van de Donk NWCJ, Stege C, Zweegman S, Nijhof IS. Carfilzomib for relapsed and refractory multiple myeloma. *Cancer Manag Res*. 2019;11:2663–75.
- Gryseels B, Mbaye A, de Vlas SJ, Stelma FF, Guissé F, van Lieshout L, et al. Are poor responses to praziquantel for the treatment of *Schistosoma mansoni* infections in Senegal due to resistance? An overview of the evidence. *Trop Med Int Health*. 2001;6:864–73.
- Hailegebriel T, Nibret E, Munshea A. Efficacy of Praziquantel for the treatment of human schistosomiasis in Ethiopia: a systematic review and meta-analysis. *J Trop Med*. 2021;2021:2625255.
- Harshbarger W, Miller C, Diedrich C, Sacchetti J. Crystal structure of the human 20S proteasome in complex with Carfilzomib. *Structure*. 2015;23:418–24.
- Horn M, Fajtová P, Rojo Arreola L, Ulrychová L, Bartošová-Sojková P, Franta Z, et al. Trypsin- and chymotrypsin-like serine proteases in *Schistosoma mansoni*—the undiscovered country. *PLoS Negl Trop Dis*. 2014;8:e2766.
- Jiang Z, Lietz CB, Podvin S, Yoon MC, Toneff T, Hook V, et al. Differential neuropeptidomes of dense core secretory vesicles (DCSV) produced at intravesicular and extracellular pH conditions by proteolytic processing. *ACS Chem Neurosci*. 2021;12:2385–98.
- Kirk CJ, Muchamuel T, Wang J, Fan RA. Discovery and early clinical development of selective immunoproteasome inhibitors. *Cells*. 2021;11:9.
- Kirkman LA, Zhan W, Visone J, Dziedzic A, Singh PK, Fan H, et al. Antimalarial proteasome inhibitor reveals collateral sensitivity from intersubunit interactions and fitness cost of resistance. *Proc Natl Acad Sci U S A*. 2018;115:E6863–70.
- Kisselev AF, Garcia-Calvo M, Overkleeft HS, Peterson E, Pennington MW, Ploegh HL, et al. The caspase-like sites of proteasomes, their substrate specificity, new inhibitors and substrates, and allosteric interactions with the trypsin-like sites. *J Biol Chem*. 2003;278:35869–77.
- LaMonte GM, Almaliti J, Bibo-Verdugo B, Keller L, Zou BY, Yang J, et al. Development of a potent inhibitor of the plasmodium proteasome with reduced mammalian toxicity. *J Med Chem*. 2017;60:6721–32.
- Lapek JD, Jiang Z, Wozniak JM, Arutyunova E, Wang SC, Lemieux MJ, et al. Quantitative multiplex substrate profiling of peptidases by mass spectrometry. *Mol Cell Proteomics*. 2019;18(5):968–81. <https://doi.org/10.1074/mcp.TIR118.001099>
- Lawong A, Gahalawat S, Ray S, Ho N, Han Y, Ward KE, et al. Identification of potent and reversible piperidine carboxamides that are species-selective orally active proteasome inhibitors to treat malaria. *Cell Chem Biol*. 2024;31:1503–1517.e19.
- Li H, O'Donoghue AJ, van der Linden WA, Xie SC, Yoo E, Foe IT, et al. Structure-and function-based design of plasmodium-selective proteasome inhibitors. *Nature*. 2016;530:233–6.
- Li H, Ponder EL, Verdoes M, Asbjørnsdóttir KH, Deu E, Edgington LE, et al. Validation of the proteasome as a therapeutic target in plasmodium using an epoxyketone inhibitor with parasite-specific toxicity. *Chem Biol*. 2012;19:1535–45.
- Li H, van der Linden WA, Verdoes M, Florea BI, McAllister FE, Govindaswamy K, et al. Assessing subunit dependency of the *Plasmodium proteasome* using small molecule inhibitors and active site probes. *ACS Chem Biol*. 2014;9:1869–76.
- Liu LJ, Francisco KR, Sun YU, Serafim MSM, Amarasinghe DK, Teixeira TR, et al. Carmaphycin B-based proteasome inhibitors to treat human African trypanosomiasis: structure–activity relationship and *in vivo* efficacy. *ACS Infect Dis*. 2024a;10(12):4182–93. <https://doi.org/10.1021/acsinfecdis.4c00441>
- Liu LJ, O'Donoghue AJ, Caffrey CR. The proteasome as a drug target for treatment of parasitic diseases. *Adv Parasitol*. 2024b;126:53–96.
- Lysyk L, Brassard R, Arutyunova E, Siebert V, Jiang Z, Takyi E, et al. Insights into the catalytic properties of the mitochondrial rhomboid protease PARL. *J Biol Chem*. 2021;296:100383.
- Madeira F, Madhusoodanan N, Lee J, Eusebi A, Niewielska A, Tivey ARN, et al. The EMBL-EBI job dispatcher sequence analysis tools framework in 2024. *Nucleic Acids Res*. 2024;52:W521–5.
- Maffioli E, Jiang Z, Nonnis S, Negri A, Romeo V, Lietz CB, et al. High-resolution mass spectrometry-based approaches for the detection and quantification of peptidase activity in plasma. *Molecules*. 2020;25:4071.
- Maurits E, Degeling CG, Kisselev AF, Florea BI, Overkleeft HS. Structure-based design of fluorogenic substrates selective for human proteasome subunits. *Chembiochem*. 2020;21:3220–4.

- McManus DP, Dunne DW, Sacko M, Utzinger J, Vennervald BJ, Zhou X-N. Schistosomiasis. *Nat Rev Dis Primers*. 2018;4:13.
- Melman SD, Steinauer ML, Cunningham C, Kubatko LS, Mwangi IN, Wynn NB, et al. Reduced susceptibility to praziquantel among naturally occurring Kenyan isolates of *Schistosoma mansoni*. *PLoS Negl Trop Dis*. 2009;3:e504.
- Mirdita M, Schütze K, Moriwaki Y, Heo L, Ovchinnikov S, Steinegger M. ColabFold: making protein folding accessible to all. *Nat Methods*. 2022;19:679–82.
- Mwanga JR, Kinunghi SM, Moshia J, Angelo T, Maganga J, Campbell CH. Village response to mass drug administration for schistosomiasis in Mwanza region, northwestern Tanzania: Are we missing socioeconomic, cultural, and political dimensions? *Am J Trop Med Hyg*. 2020;103:1969–77.
- Nagle A, Biggart A, Be C, Srinivas H, Hein A, Caridha D, et al. Discovery and characterization of clinical candidate LXE408 as a kinetoplastid-selective proteasome inhibitor for the treatment of leishmaniasis. *J Med Chem*. 2020;63:10773–81.
- O'Donoghue AJ, Bibo-Verdugo B, Miyamoto Y, Wang SC, Yang JZ, Zuill DE, et al. 20S proteasome as a drug target in *Trichomonas vaginalis*. *Antimicrob Agents Chemother*. 2019;63(11):e00448-19. <https://doi.org/10.1128/aac.00448-19>
- O'Donoghue AJ, Eroy-Reveles AA, Knudsen GM, Ingram J, Zhou M, Statnikov JB, et al. Global identification of peptidase specificity by multiplex substrate profiling. *Nat Methods*. 2012;9:1095–100.
- O'Donoghue AJ, Liu C, Simington CJ, Montermoso S, Moreno-Galvez E, Serafim MSM, et al. Comprehensive proteolytic profiling of *Aedes aegypti* mosquito midgut extracts: unraveling the blood meal protein digestion system. *PLoS Negl Trop Dis*. 2025;19(2):e0012555. <https://doi.org/10.1371/journal.pntd.0012555>
- O'Donoghue AJ, Knudsen GM, Beekman C, Bennett RJ. Destructin-1 is a collagen-degrading endopeptidase secreted by *Pseudogymnoascus destructans*, the causative agent of white-nose syndrome. *Proc Natl Acad Sci U S A*. 2015;112:7478–83.
- Potts BC, Albitar MX, Anderson KC, Baritaki S, Berkers C, Bonavida B, et al. Marizomib, a proteasome inhibitor for all seasons: preclinical profile and a framework for clinical trials. *Curr Cancer Drug Targets*. 2011;11(3):254–84. <https://doi.org/10.2174/156800911794519716>
- Ramirez KG. Ixazomib: an oral proteasome inhibitor for the treatment of multiple myeloma. *J Adv Pract Oncol*. 2017;8:401–5.
- Robbertse L, Fajtová P, Šnebergerová P, Jalovecká M, Levytska V, Barbosa da Silva E, et al. Evaluating antimalarial proteasome inhibitors for efficacy in *Babesia* blood stage cultures. *ACS Omega*. 2024;9:44989–99.
- Rohweder PJ, Jiang Z, Hurysz BM, O'Donoghue AJ, Craik CS. Multiplex substrate profiling by mass spectrometry for proteases. *Methods Enzymol*. 2023;682:375–411.
- Roth P, Gorlia T, Reijneveld JC, de Vos F, Idbaih A, Frenel JS, et al. Marizomib for patients with newly diagnosed glioblastoma: a randomized phase 3 trial. *Neuro Oncol*. 2024;26:1670–82.
- Rut W, Poręba M, Kasperkiewicz P, Snipas SJ, Drag M. Selective substrates and activity-based probes for imaging of the human constitutive 20S proteasome in cells and blood samples. *J Med Chem*. 2018;61:5222–34.
- Sabah AA, Fletcher C, Webbe G, Doenhoff MJ. *Schistosoma mansoni*: chemotherapy of infections of different ages. *Exp Parasitol*. 1986;61:294–303.
- Sahu I, Glickman MH. Proteasome in action: substrate degradation by the 26S proteasome. *Biochem Soc Trans*. 2021;49:629–44.
- Schots R, Fostier K, De Becker A. Carfilzomib: a novel treatment in relapsed and refractory multiple myeloma. *Onco Targets Ther*. 2012;5:237–44. <https://doi.org/10.2147/OTT.S28911>
- Small JL, O'Donoghue AJ, Boritsch EC, Tsodikov OV, Knudsen GM, Vandal O, et al. Substrate specificity of MarP, a periplasmic protease required for resistance to acid and oxidative stress in *Mycobacterium tuberculosis*. *J Biol Chem*. 2013;288:12489–99.
- Summers S, Bhattacharyya T, Allan F, Stothard JR, Edielu A, Webster BL, et al. A review of the genetic determinants of praziquantel resistance in *Schistosoma mansoni*: Is praziquantel and intestinal schistosomiasis a perfect match? *Front Trop Dis*. 2022;3:933097.
- Toste Rêgo A, da Fonseca PCA. Characterization of fully recombinant human 20S and 20S-PA200 proteasome complexes. *Mol Cell*. 2019;76:138–147.e5.
- Verdoes M, Florea BI, Menendez-Benito V, Maynard CJ, Witte MD, van der Linden WA, et al. A fluorescent broad-spectrum proteasome inhibitor for labeling proteasomes in vitro and in vivo. *Chem Biol*. 2006;13:1217–26.
- Verjee MA. Schistosomiasis: still a cause of significant morbidity and mortality. *Res Rep Trop Med*. 2019;10:153–63.
- Waterhouse AM, Procter JB, Martin DMA, Clamp M, Barton GJ. Jalview version 2—a multiple sequence alignment editor and analysis workbench. *Bioinformatics*. 2009;25:1189–91.
- WHO. Schistosomiasis. 2023. Available from: <https://www.who.int/news-room/fact-sheets/detail/schistosomiasis>
- Winter MB, la Greca F, Arastu-Kapur S, Caiazza F, Cimermancic P, Buchholz TJ, et al. Immunoproteasome functions explained by divergence in cleavage specificity and regulation. *eLife*. 2017;6:27364.
- Wolfe AR, Neitz RJ, Burlingame M, Suzuki BM, Lim KC, Scheideler M, et al. TPT sulfonate, a single, oral dose schistosomicidal prodrug: in vivo efficacy, disposition and metabolic profiling. *Int J Parasitol Drugs Drug Resist*. 2018;8:571–86.
- Wyllie S, Brand S, Thomas M, de Rycker M, Chung CW, Pena I, et al. Preclinical candidate for the treatment of visceral leishmaniasis that acts through proteasome inhibition. *Proc Natl Acad Sci U S A*. 2019;116:9318–23.
- Xie SC, Gillett DL, Spillman NJ, Tsu C, Luth MR, Ottilie S, et al. Target validation and identification of novel boronate inhibitors of the *Plasmodium falciparum* proteasome. *J Med Chem*. 2018;61:10053–66.
- Yoo E, Stokes BH, de Jong H, Vanaerschot M, Kumar TRS, Lawrence N, et al. Defining the determinants of specificity of *plasmodium* proteasome inhibitors. *J Am Chem Soc*. 2018;140:11424–37.
- Zwang J, Olhario P. Efficacy and safety of praziquantel 40 mg/kg in preschool-aged and school-aged children: a meta-analysis. *Parasit Vectors*. 2017;10:47.

SUPPORTING INFORMATION

Additional supporting information can be found online in the Supporting Information section at the end of this article.

How to cite this article: Silva EB, Jiang Z, Liu C, Fajtová P, Teixeira TR, de Castro Fiorini Maia G, et al. Enhancing schistosomiasis drug discovery approaches with optimized proteasome substrates. *Protein Science*. 2025;34(6):e70180. <https://doi.org/10.1002/pro.70180>